

Analyzing CMB B-map using the Minkowski Functionals

Yangrui Hu

Room 206, Building #320, No.96 Jinzhai Road, USTC, Hefei, Anhui, P, R, China
hyr1996@mail.ustc.edu.cn

Abstract

The detection of the magnetic type B-mode polarization is the main goal of future cosmic microwave background (CMB) experiments. In the standard model, the B-mode map is a strongly non-gaussian field due to the cosmic weak lensing effect component. Besides the two-point correlation function, the other statistics are also very important to dig the information of the polarization map. In this poster, the Minkowski functionals (MFs) are employed to study the morphological properties of the lensed B-mode maps by comparing the results with Gaussian map. Additionally, in order to investigate the leakage from E-mode to B-mode, we set up both real case and ideal case to compare.

Introduction

The temperature and polarization anisotropies of the cosmic microwave background (CMB) radiation contain useful cosmological information and play a crucial role in constraining cosmological parameters, as well as testing the cosmological principle in modern cosmology. In the standard cosmological model, the CMB is a linearly polarized photon field, which is completely described by the stocks parameters, Q and U. However, the Stokes parameters depend on the arbitrary choice of coordinates. It is then convenient to define the electric-type (i.e. E-mode) and magnetic-type (i.e. B-mode) polarization fields from the observables Q and U.

The linear polarization parameters Q&U, complex conjugate polarisation fields P and E&B are defined as follows:

$$P_{\pm}(\hat{\gamma}) \equiv Q(\hat{\gamma}) \pm iU(\hat{\gamma}) = \sum_{lm} a_{\pm 2,lm} \pm 2Y_{lm}$$

$$E(\hat{\gamma}) \equiv \sum_{lm} E_{lm} Y_{lm}(\hat{\gamma}), E_{lm} \equiv -\frac{1}{2}[a_{2,lm} + a_{-2,lm}], B(\hat{\gamma}) \equiv \sum_{lm} B_{lm} Y_{lm}(\hat{\gamma}), B_{lm} \equiv -\frac{1}{2i}[a_{2,lm} - a_{-2,lm}]$$

where $\hat{\gamma}$ denotes the position, Y_{lm} are the spin-weighted spherical harmonics.

The B-mode polarization is generated by different sources. First, primordial gravitational waves, predicted by inflationary theories, can generate primordial B-mode signal on CMB. Second, the cosmic weak lensing generates non-cosmological B-mode signal due to the CMB photons scatter by galaxies in the path from the Last Scattering Surface to us. Leakage is another source of B-mode due to the unavoidable sky cut during the data analysis. Because of the Galactic foreground, we can't use the full-sky data, therefore we must cut the part of sky which is dominated by the signal of our galaxy. To obtain E-mode and B-mode from Q and U observables after cutting sky, there is leakage from E-mode to B-mode that contaminates the data. Finally, foregrounds can also contribute to the B-mode signal. In my work, I deal with only two of these cases of B-mode signal: CMB lensing and leakage.

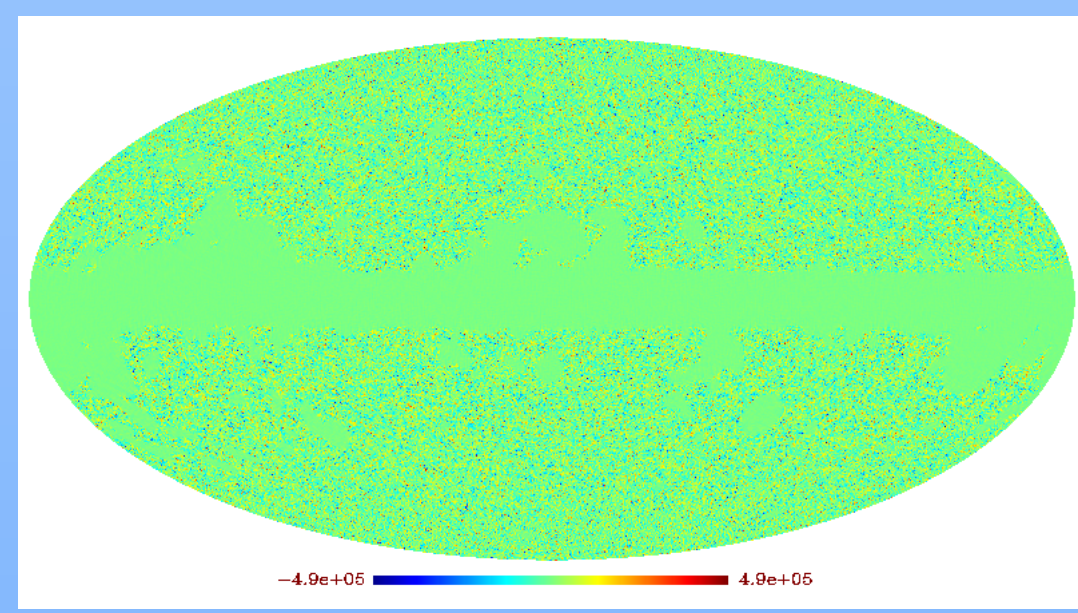


Figure 1: B-mode map (Lensing)

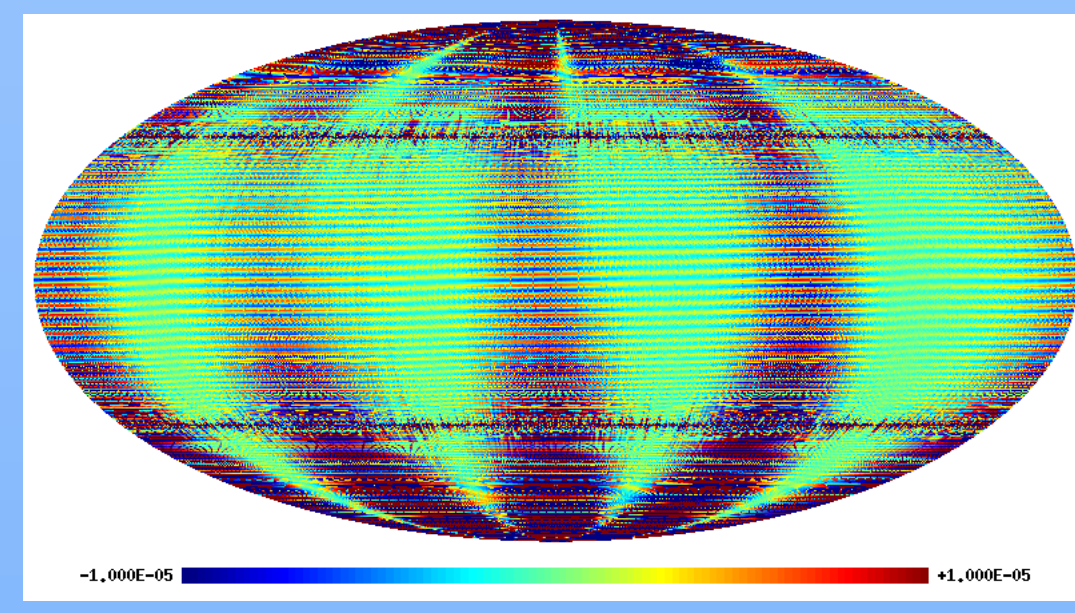


Figure 2: Leakage

Simulations

Here, we do 1000 simulations to analyze the B-mode signal. The steps to obtain the simulations are as follow:

Step1. Use CAMB to generate power spectrum with $r=0$, which means that there is no primordial B-mode.

Step2. Generate T,Q,U maps using Lenspix (lensed non-Gaussian maps) and Healpix (Gaussian maps).

Step3. For the real case, we cut the sky of Q and U maps using smoothed Planck mask, then generate non-Gaussian B-maps. The Gaussian smoothing function leaves the least leakage comparing with cos and sin smoothing function, therefore we use the Gaussian function to smooth the mask.

For the ideal case, we first generate the B-maps, then, finally, cut the sky.

Since in CAMB we set $r=0$, the B-mode should only come from lensing in the ideal case, and lensing+ leakage in the real case.

Step4. Use gaussian beam to smooth the final B-maps (lensed and gaussian) both in real and ideal cases. In my simulations, the parameter of the gaussian beam is $\theta_s = 60'$

Step5. Calculate the Minkowski functionals for every B-map.

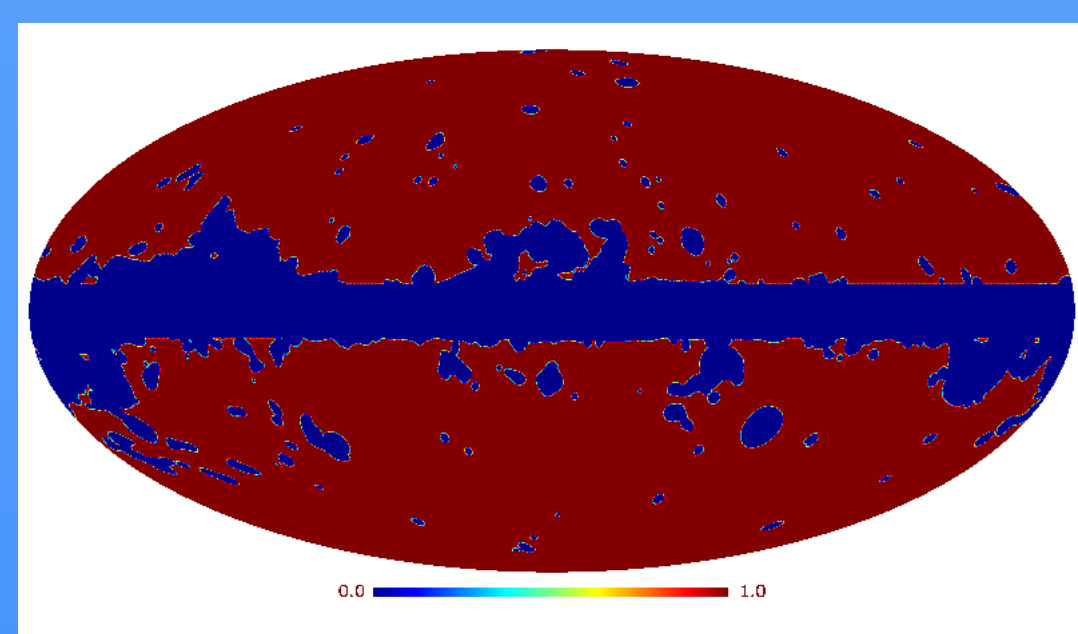
Step6. Compare the results.

Figure 3: Gaussian smoothed planck mask.

This figure is the smoothed mask I used to cut the sky. The Gaussian smoothing function is defined as:

$$W_i = \begin{cases} \int_{-\infty}^{\delta_i - \frac{\delta_c}{2}} \frac{1}{\sqrt{2\pi\sigma^2}} \exp\left(-\frac{x^2}{2\sigma^2}\right) dx = \frac{1}{2} + \frac{1}{2} \text{erf}\left(\frac{\delta_i - \frac{\delta_c}{2}}{\sqrt{2}\sigma}\right) & \delta_i < \delta_c \\ 1 & \delta_i > \delta_c \end{cases}$$

Smoothing range equals 1 degree and the jump range equals 10^{-6} .



Minkowski Functionals (MFs)

- > MFs describe the morphological features of random fields over excursion sets
- > Any morphological property can be expanded as a linear combination of three MFs.
- > Consider a smooth scalar field $u(x)$. For a given threshold ν , define the excursion set Q and its boundary ∂Q of a smooth scalar field u as follows:

$$Q_{\nu} = \{x \in S^2 | u(x) > \nu\}, \quad \partial Q_{\nu} = \{x \in S^2 | u(x) = \nu\}$$

- > The definition of three Minkowski functionals in 2-dimensional sphere:

$$\begin{cases} v_0(\nu) = \int_{Q_{\nu}} \frac{dA}{4\pi} & \text{first MF, } \nu \text{ is threshold} \\ v_1(\nu) = \int_{\partial Q_{\nu}} \frac{dl}{16\pi} & \text{second MF} \\ v_2(\nu) = \int_{\partial Q_{\nu}} \frac{\kappa dl}{8\pi^2} & \text{third MF, } \kappa \text{ is geodesic curvature} \end{cases}$$

Results

Real case :

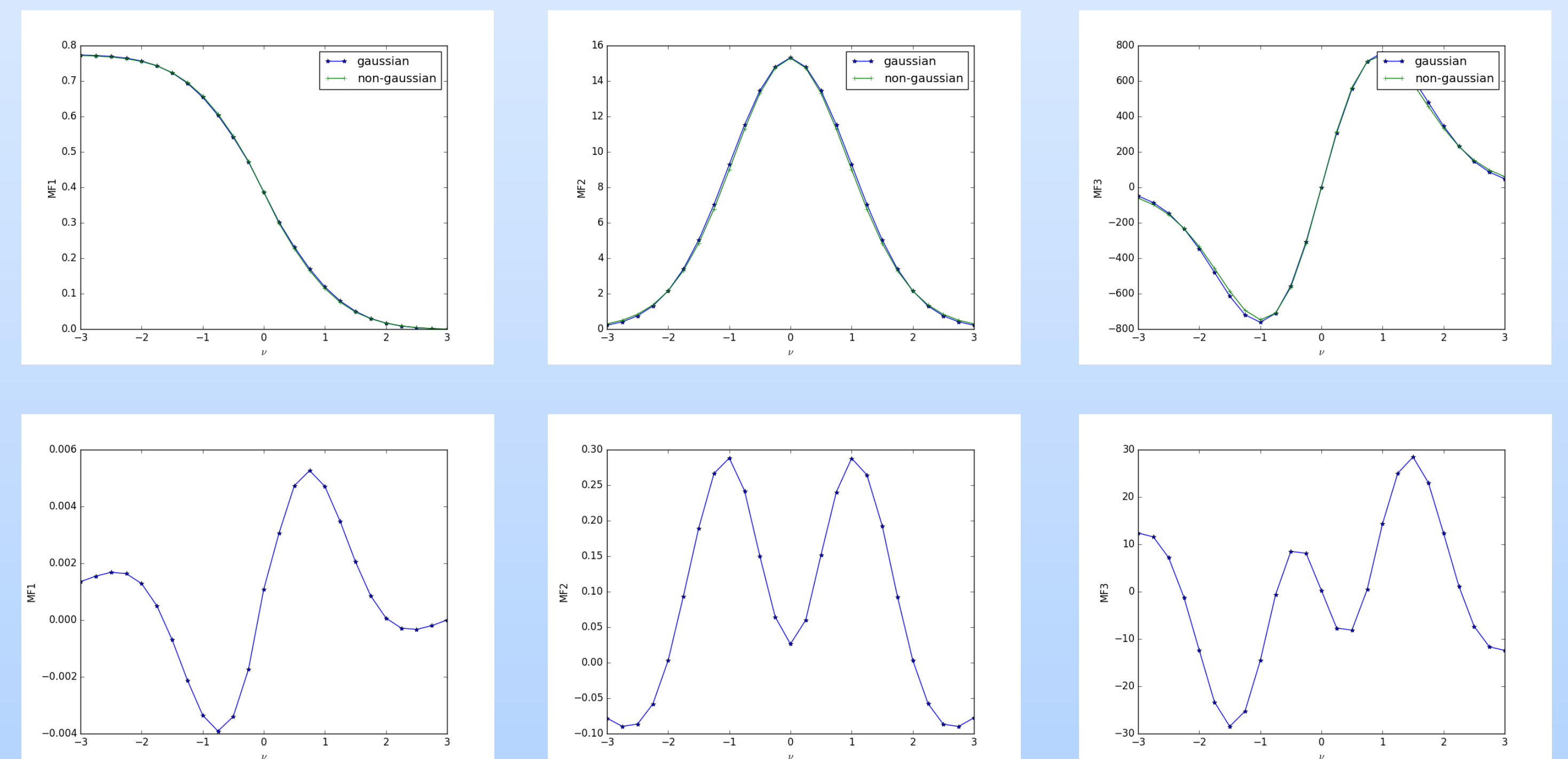


Figure 4: Three MFs for the real case. The figures in the top row, from left to right, are, respectively, the first, the second and the third MF. In each figure, I plot the gaussian and non-gaussian results together. Three figures in the bottom row are the difference between the gaussian curves and the non-gaussian ones for each MF.

Ideal case:

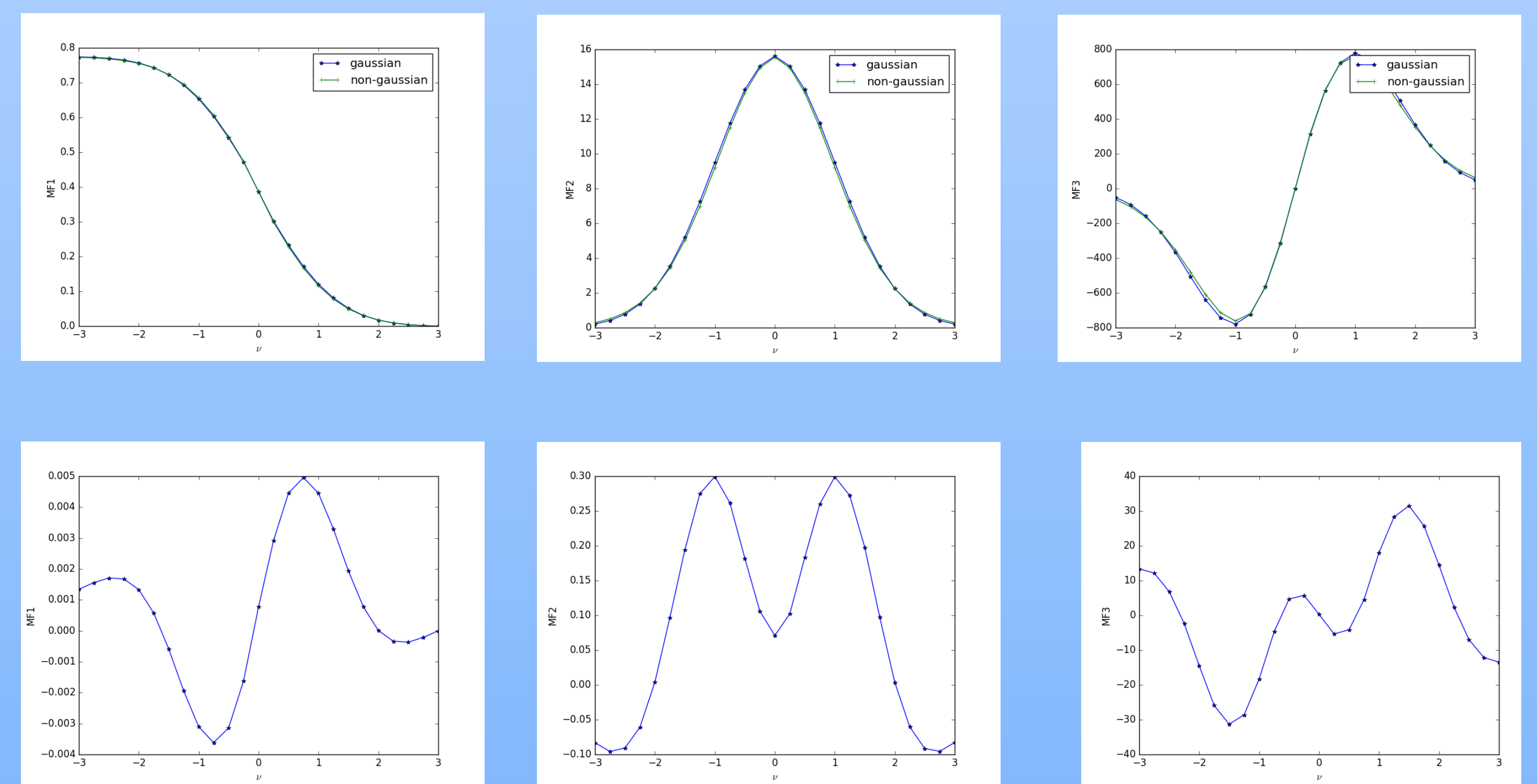


Figure 5: Three MFs for the ideal case. Three figures in the top row, from left to right, are, respectively, the first, the second and the third MF. In each figure, I plot the gaussian and non-gaussian results together. The three figures in the bottom row are the difference between the gaussian curves and the non-gaussian ones for each MF.

Non-gaussian results comparison:

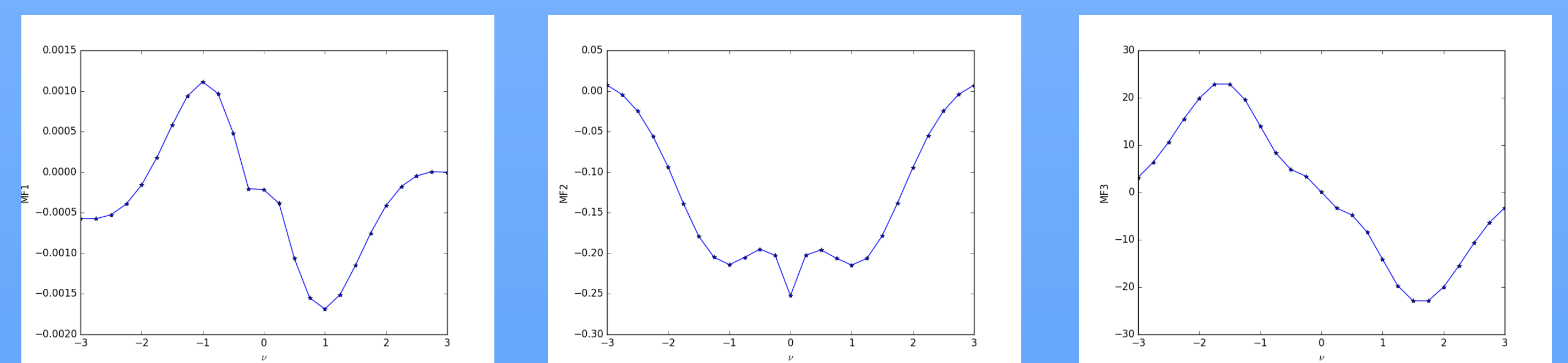


Figure 6: Three figures are the difference of non-gaussian results between real case and ideal case. From left to right, respectively, the first, the second and the third MF.

Conclusion:

In the standard cosmological model, T and E are excellent random Gaussian fields according to the linear theory. However the B-mode should be a strong non-gaussian field due to cosmic weak lensing effect. In addition to the two-point correlation function, some other statistics are important too, such as Minkowski functional that contains a complementary information of the B-mode field.

In this poster, we employ MFs to probe the topological properties of lensed B-mode polarization map. We find that the B-map definitely deviates from Gaussianity, comparing with Gaussian fields. For partial sky surveys, the non-gaussianity can be detected well. In our simulation, we do not consider noise. For the real case and ideal case, there are some differences in the results, due to the leakage from E-mode to B-mode. In the real case there is leakage, on the other hand, B-mode in the ideal case only comes from lensing.

Acknowledgements:

I acknowledge the use of the Planck Legacy Archive (PLA). Our data analysis was done using the HEALPix, CAMB and LensPix. I also acknowledge Larissa Santos, Kai Wang and Jarready K. for helpful discussions.

References :

- [1]. W. Zhao, L. Santos. Probing the statistical properties of CMB B-mode polarization through Minkowski Functionals, arXiv:1510.07779v1
- [2]. A. Ducout, F. R. Bouchet, S. Colombi, D. Pogosyan and S. Prunet. Non Gaussianity and Minkowski Functionals: forecasts for Planck, arXiv:1209.1223v1
- [3]. Yi-Fan Wang, Kai Wang, Wen Zhao. Smoothing methods comparison for CMB E- and B-mode separation, arXiv:1511.01220v1
- [4]. Kendrick M. Smith, Pseudo-C estimators which do not mix E and B modes, arXiv:astro-ph/0511629v2
- [5]. Gorski, K. M., Hivon, E., Banday, A., et al. 2005, The Astrophysical Journal, 622, 759
- [6]. <http://camb.info/>; A. Lewis, A. Challinor and A. Lasenby, Astrophys. J. 538, 476 (2000).
- [7]. <http://cosmologist.info/lenspix/>; A. Lewis, Phys. Rev. D 71, 083008 (2005).